Considerations for Bilge Keel Force Models in Potential Flow Simulations of Ship Maneuvering in Waves

Christopher Bassler, Ronald Miller, Arthur Reed

David Taylor Model Basin (NWSC/CD)

Alan Brown

Virginia Tech

ABSTRACT

Requirements for ship operations, both naval and commercial, may result in increased exposure to heavy weather and the occurrence of large amplitude motions. In order to enable evaluation of hull form designs, or to develop detailed ship specific operator guidance for these critical conditions, potential flow sectional, or strip-theory based, approaches remain the most practical method for fast ship motions simulations. However, some essential physical effects regarding the bilge keels may not be captured by the potential flow sectional formulations. To examine the relative importance of these effects, a series of unsteady RANS (URANS) computations were performed for the ONR Tumblehome model experiencing large amplitude roll motion at both zero and forward speed conditions, in calm water and in waves.

KEYWORDS

Bilge keels, potential flow, large amplitude motions

INTRODUCTION

Since their introduction in the mid-19th century, bilge keels remain an important hull form feature to increase damping and reduce the severity of roll motions experienced by a ship in waves (e.g. Froude, 1865; Bryan, 1900; Martin, 1958; Kato, 1965). This passive means of mitigating roll motion has become common for ships. Despite their importance, bilge keel models, particularly in fast numerical simulations using potential flow methods (cf. Beck & Reed, 2001), are often simplified. Because of this, they are not necessarily accurate in heavy weather sea conditions, where the bilge keels are important for reducing the likelihood of large roll motions.

Potential flow methods for ship motions assessment depend on accurate modeling of roll damping to determine ship roll motion. However, the traditional semi-empirical roll damping models (Ikeda, et al., 1978; Himeno, 1981) do not explicitly account for the physical phenomena which occur during large amplitude ship motions, including the reduced effectiveness of the bilge keels (Bassler & Reed, 2009; Reed, 2009; Bassler, et al., 2010a, 2010b, 2011). Unless the bilge-keel model adequately captures the primary physical forces, ship motions may not be predicted accurately enough for design assessments or for the development of ship-specific operator guidance.

In order to obtain more accurate predictions of ship roll motion, high-fidelity codes may also be used. Improvements have been made in roll damping predictions using viscous flow codes (Yeung, et al., 1998, 2000; Roddier, et al., 2000; Seah, 2007; Seah & Yeung, 2008) and URANS codes (Korpus & Falzarano, 1997; Miller, et al., 2002, 2008; Wilson, et al., 2006). However, currently, their computational requirements prevent their expansive use for early-stage design assessments, or assessments for a large number of conditions.

The roll motion of a ship is influenced by both its shape and appendages. Viscous related phenomena, such as flow separation from the bilge, skeg and bilge keels with the subsequent vortex formation, account for a large portion of

roll damping. Bilge keels also generate a lift force with forward motion of the ship, which further tends to dampen the roll motion. For new ship designs, the effectiveness of the bilge keels for damping roll motion needs to be determined for a large range of roll angles and ship speeds.

Several important considerations are often neglected in the numerical tools that are needed for early-stage design evaluation, or to compute large numbers of realizations to develop ship-specific operator guidance. These include reduced effectiveness of bilge keels during large amplitude roll motion, the effectiveness of bilge keels while maneuvering in waves, and considerations for energy dissipation through shed vorticity from the bilge keels during these conditions.

Recent advances consider the effects of large amplitude motions for numerical ship motion performance assessments (e.g. Belknap & Reed, 2010; Belknap, et al., 2010). These advances have focused on the development and expansion of models for potential flow simulation tools with sectional formulations. However, additional effects of bilge keels due to vortex shedding, flow convection downstream, waves, and bilge keel emergence and submergence during large roll motion may be important, but not necessarily accounted for in the sectional formulations.

A series of unsteady Reynolds Averaged Navier Stokes (URANS) computations were performed for both 2-D and 3-D conditions of large amplitude ship roll motion, with and without forward speed, and in calm water and in waves. Comparisons were made to available experimental data for the 2-D calm water conditions at zero-speed. These results were then compared to the 3-D conditions to develop improved understanding of additional physical effects, including forward speed and waves, which should be considered for future developments of strip-theory approaches for ship motions prediction.

The purpose of this study was to examine high-fidelity numerical bilge keel force results and assess the relative importance of the additional physical effects which may need to be considered in future developments of sectional force component models for bilge keels. Some potential issues for modeling these effects in bilge keel force models are also discussed.

BILGE KEEL FORCE MODELS

Existing bilge keel force models are typically based on a Morison-equation type formulation, or more advanced bilge keel models which consider unsteady vortex shedding. Both types of models are briefly discussed. However, there is still a need to improve these models, with consideration for large amplitude roll motions. Currently, bilge-keel force models using either the zero-speed (Morison-equation based) or forward speed formulations do not consider the physical phenomena which occur during large amplitude roll motions.

Morison-Equation Based Models

The Morison equation (Morison, et al., 1950, 1953) is a robust engineering formulation for drag/inertia dominated problems of a body in an oscillatory fluid. However, it has limited application due to its semi-empirical form and its basis of using harmonically oscillating planar motion. The semi-empiricism requires precision in selecting values for the inertia and drag coefficients. For applications in non-harmonically oscillating fluids, such as ship motions in irregular waves, application of this method may be limited. Morison's equation appears to be most appropriate for conditions where the Keulegan-Carpenter number is less than 8, or greater than 25 (Sarpkaya & Isaacson, 1981). Keulegan & Carpenter (1958) were the first to attempt to improve on the Morison equation, by specifying a remainder value, while still neglecting diffraction effects. Additional modifications have included consideration of higher-order harmonics (Sarpkaya, 1981).

A Morison-equation-type formulation was used to study oscillating flow around 2-D and 3-D bilge keels, as represented by flat plates (Sarpkaya & O'Keefe, 1996). However, wall effects that may be significant are not accounted for in typical flat plate formulations. Additional studies were carried out to examine the hydrodynamic forces on flat plates in forced oscillation (Klaka, *et al.*, 2007).

The unit normal force on the bilge keel can be modeled, using a Morison-type equation, as the sum of viscous drag and added mass due to roll motion. Initial models for the bilge keel force only considered the drag induced force on the bilge keel for zero speed (Lloyd, 1998; Themelis, 2008).

However, even for zero speed conditions, the bilge keel force still retains some component due to added mass effects, particularly for thick span bilge keels.

A similar bilge keel force model formulation to describe the force on the bilge keel during roll decays was detailed in Irvine, et al. (2006). This formulation was expanded with a suggested possible forward speed correction in Atsavapranee, et al. (2007) and with considerations for multiple degree-of-freedom (roll and heave) motions and the effects of wave orbital velocities in Grant, et al. (2007).

Potential flow ship motions codes typically use some variation of Ikeda's bilge keel component (Ikeda, et al., 1978), which considers the bilge keel force as a combination of the normal force component and the hull interaction component and neglects wave-making due to the bilge keel, which may be significant for large amplitude roll motion (Bassler & Reed, 2009).

Unsteady Lifting Surface Models

Additional models for potential flow codes have been developed using unsteady lifting surface theory, based on a vortex-lattice method. Liut (1999) and Liut & Lin (2006) used a vortex-lattice method to model arbitrary lifting shapes, such as rudders and fins. This is the approach applied in the *Large Amplitude Motions Program* (LAMP), and considers the lift force on the bilge keels (Lin & Yue, 1990; Lin, et al., 2006). Additionally, if the lifting surface stalls, then an eddy-making force is computed. This is equivalent to the force on a flat plate, with the flow normal to the surface of the plate. The typical angle of stall considered for the bilge keels is 12 deg.

Greeley & Petersen (2010) developed a bilge keel force model using an unsteady lifting surface (ULS) approach and showed favorable comparisons to the experimental and RANS results given in Miller, et al. (2002) for a 3-D circular cylinder with instrumented bilge keels. In order to expand the application of this model to low speed conditions, the ULS model was coupled with a Morison-equation based approach for very low speeds and the bilge keel force is obtained by switching between the two models, depending on the speed conditions. This formulation is currently utilized in the potential flow ship motions code TEMPEST (Belknap & Reed, 2010).

Large Amplitude Roll Models

For large amplitude ship roll motion, the bilge keels may become less effective, due to their interaction with the free surface and, for more severe motions, due to possible emergence. To further investigate the physical phenomena which occur during large amplitude roll motion, and to improve the modeling of these conditions in strip-theory based approaches, a series of experiments were performed (Bassler, et al., 2010b) for a 2-D midship section model (DTMB Model 5699) derived from the ONR Topside Series hull forms (Bishop, et al., 2005). These experiments used instrumented bilge keels to measure the force on the bilge keels through the forced roll oscillations, including conditions where large amplitude roll resulted in bilge keel emergence.

From the experiments, abrupt changes in the geometry of the body relative to the free surface were observed, which must be considered to accurately determine the properties of the dynamical system modeling ship roll motion (Bassler, et al., 2010a). Because existing theoretical models were developed for small to moderate roll motions, the amount of energy dissipation for large amplitude roll motion may be over-estimated, resulting in under-predicted roll motion (Bassler & Reed, 2009; Reed, 2009).

In order to consider these physical phenomena in models for ship roll damping, and increase their applicability and robustness, a piecewise formulation for total ship roll damping was proposed (Bassler, et al., 2010a, 2011). However, the piecewise model represented a simplified approach to the consideration of large amplitude effects for ship roll motion. For more accurate modelling, especially for more advanced potential flow numerical tools with discrete force models (e.g. Belknap & Reed, 2010), an explicit model for the bilge keel force, with the consideration of large amplitude roll motion effects may be used.

URANS SIMULATIONS

To examine the relative importance of the physical effects identified earlier, a series of Unsteady Reynolds Averaged Navier Stokes (URANS) computations were performed.

Solver

Calculations were performed using the URANS solver CFDShip-Iowa, Version 4. CFDShip-Iowa is a general-purpose research RANS computational fluid dynamics code developed at the University of Iowa.

Basic solver numerical modeling details include 2nd-order upwind convective terms and 2nd-order central differenced viscous terms. For time discretization a 2nd-order backward difference scheme is used. CFDShip-Iowa uses predictor/corrector algorithms to couple the velocity and pressure and to enforce continuity. Turbulence modelling uses the blended k-ε/k-ω model of Menter (1994). The solver uses Message Passing Interface (MPI)-based domain decomposition for parallel processing. Details of the solution algorithm and numerical methods can be found in numerous references, including Carrica, et al. (2006, 2007a, 2007b). Details on previous applications of the code to problems of roll motion and bilge keel forces can be found in Miller, et al. (2002, 2008).

Dynamic Overset Grids

CFDShip-Iowa uses dynamic overset grids to allow for the relative motion between blocks of meshes. Overset grids are used in a wide variety of applications, including calculations of a static hull embedded in a background grid and dynamically moving, fully-appended ships. Additionally, overset grids remove the necessity of point-to-point matching in structured grid systems. This capability alleviates some of the difficulties involved in creating structured grids for complex configurations, such as hulls appended with shafts and struts. The grid assembling tool SUGGAR (Structured Unstructured Generalized Grid Assembler), Version 2.73 (Noack 2005) was used.

SUGGAR may be run as a preprocessor for static calculations, or concurrently with CFDShip-Iowa, using calls to subroutines. The software, USURP, Version 2.39, (Boger & Dreyer, 2006), was used to properly compute area and forces on overlapping surface regions.

For the calculations presented in this paper fixed yaw angles (±10 deg) and single degree-of-freedom (1-DoF) roll motion were prescribed, and a constant forward speed was imposed using uniform inflow into the computational domain. The axis of rotation was along the ship's center plane, through the vertical center of gravity. The body sway, heave, pitch, and yaw modes of motion were fixed for the 1-DoF roll calculations. At each time-step, the solver obtained the motion and sent the information to SUGGAR to create new grid assembling information. CFDShip-Iowa's implicit motion solver was utilized, resulting in updated grid motion at every inner-iteration of the time-step solution. Typically 3 to 5 inner iterations were performed at each time step. At each time step, CFDShip-Iowa uses the new value of roll displacement to re-orient the ship. SUGGAR was then run to update the grid assembly for the new orientation.

Overlapping boundary fitted grids were created for the port and starboard sides of the hull and the port and starboard bilge keel grids. A cross-section of the grid assembly shows the relative grid point densities of the hull, refinement, and background grids (Fig. 1), and also illustrates the use of dynamic overset grids. The moving hull grid assembly was embedded in a stationary intermediate refinement grid, which was embedded in a larger stationary background grid, representing a towing tank. The intermediate refinement grid is used to blend the grid sizes of the very fine boundary layer grid with the coarser background grid. As the hull grid rotates relative to the fixed background grids, new grid connectivity information is calculated by SUGGAR.

Computational Domain

The computational region is shown in Fig. 2. The surface discretization of the hull appended with bilge keels is shown in Fig. 3. No-slip boundary conditions were applied to the hull and appendages, far-field boundary conditions were applied to the side and bottom walls. A constant inlet velocity, $U/U_{ref} = U_S$, $V/U_{ref} = 0$ and $W/U_{ref} = 0$, represents the constant forward speed (Fig. 4). The velocities are extrapolated at the exit.

Details of the computational grid size are given in Table 1. The total number of grid points used for the URANS simulations was about 4.8 million. The skeg was integrated into the hull grid. The domain was decomposed into 45 smaller blocks for parallel processing. One additional processor was used for SUGGAR.

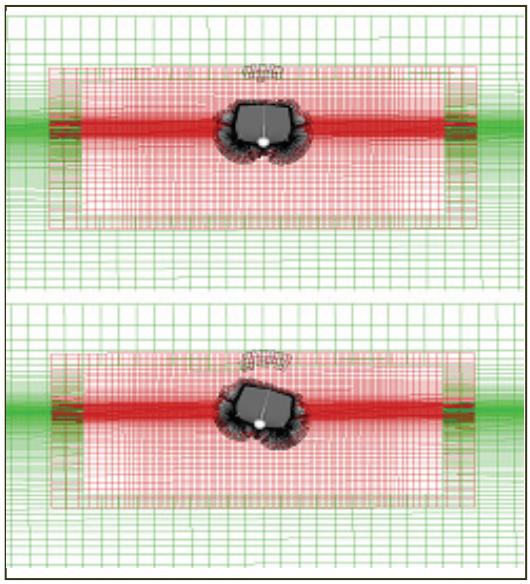

Fig.1. SUGGAR grid assembly for DTMB Model 5613-1 at two roll positions, with relative grid densities between refinement and background grids.

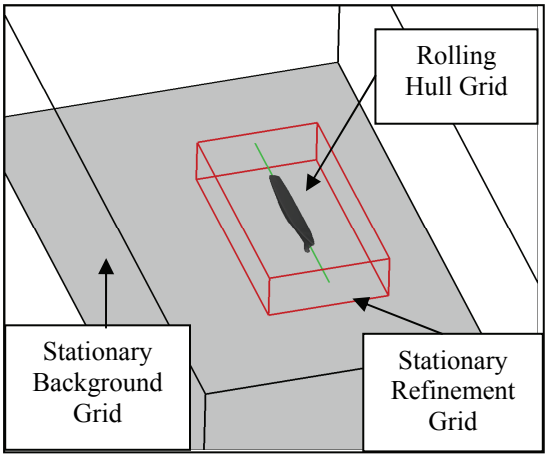

Fig.2. Computational region: moving hull, grid, stationary refinement, and background grids.

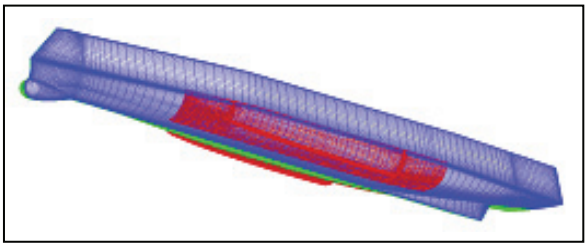

Fig.3. Hull and bilge keels surface discretizations, shown for DTMB Model 5613-1.

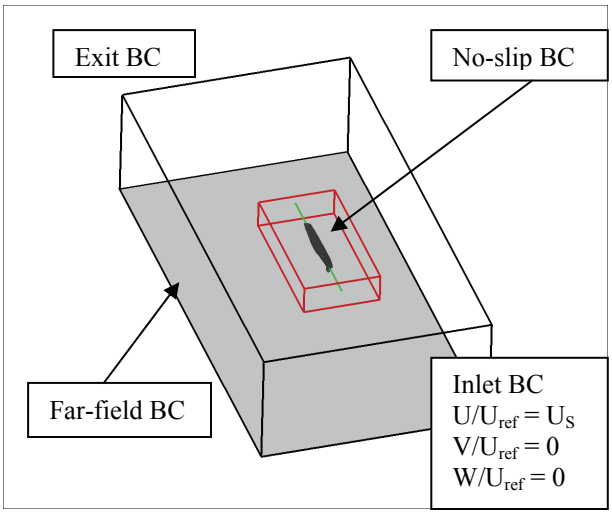

Fig.4. CFDShip-Iowa boundary conditions.

Obtaining Segmented Forces on the Bilge Keel

CFDShip-Iowa sums the force/moment contributions from all of the wetted wall surface elements at each time step. In order to obtain segmented forces on the bilge keel, a post-processing routine was developed to create longitudinal segments distributions, Δx, over the hull and appendages. By decomposing the total force on all the wetted surface elements at each time step into these longitudinal segments, a force/Δx is obtained at each specified x location segment (Fig. 5).

Table 1. DTMB Model 5613-1 grid sizes and decomposition.

Block	# pts.	# proc.	# pts/proc.
Hull Stb	667,116	6	111,186
Hull Prt	667,116	6	111,186
BK Stb	363,750	3	121,250
BK Prt	363,750	3	121,250
Refinement	1,519,035	15	101,269
Background	1,241,240	12	103,436
Total	4,822,007	45	Avg = 107,155

The development of this post-processing routine[3] enabled changes to be made to the constraints, which do not necessarily conform to the surface

[3] This routine was developed by Miller at NSWCCD in 2010.

meshes, or the regions of interest on the hull form, after the simulations have been performed without having to re-run them. Local regions, such as pressures on the bow dome or forces on the appendages (bilge keels, rudders, shafts, struts) may then be determined.

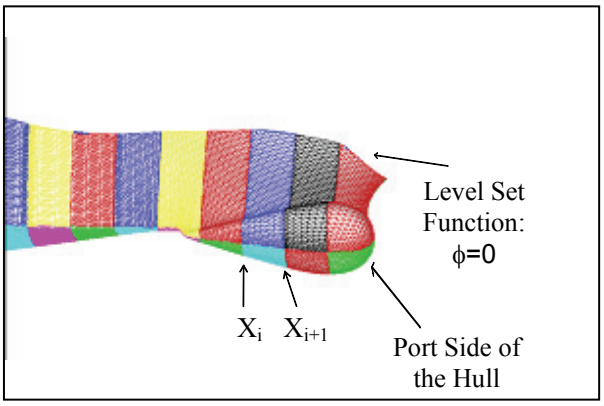

Fig. 5: Post-processing example of longitudinal segments for the hull, with the bow section shown, up to the instantaneous waterline

Hull Form and Simulated Conditions

Simulations were performed for both a 2-D and 3-D hull form. The ONR Topside Series, tumblehome topside configuration hull (Bishop, et al., 2005) was used (Table 2). A 32nd scale model, DTMB Model 5613-1, had been used for previous experiments (Bassler, et al., 2007) and simulations (Miller, et al., 2008) of forced roll motions. A 2-D midship section model of this hull form (Fig. 6), DTMB Model 5699-1, was also constructed at the same scale ratio to carry out sectional experiments of large amplitude roll motion (Bassler, et al., 2010b) and enable comparisons to the 3-D model at the same scale ratio. For simulations of DTMB Model 5613-1, 20 segments were specified (Fig. 7) to interrogate the bilge keel force during the prescribed roll motions.

Simulations were performed for forced 1-DoF roll motions, moderate to large amplitude, in calm water at zero speed and with forward speed. Additionally, simulations were performed in beam sea regular waves, with wavelength equal to ship length and a steepness of 1/100, for zero speed, and for steady drift in calm water at forward speed (Table 3).

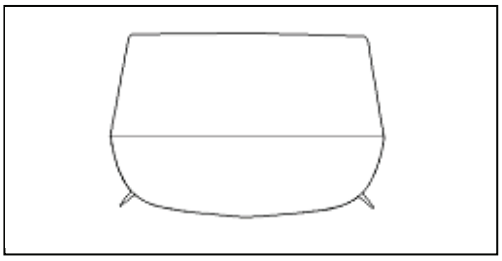

Fig. 6. Midship section of the ONR Topside Series, Tumblehome configuration hull form with bilge keels (DTMB Model 5699-1)

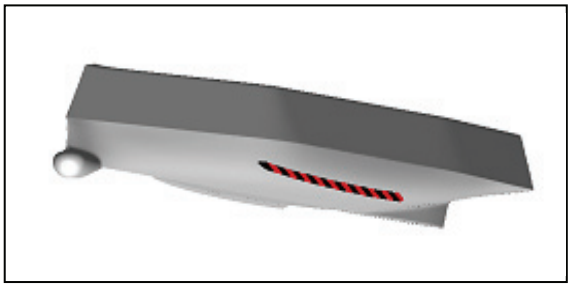

Fig. 7 DTMB Model 5613-1 with bilge keel divided into 20 segments for sectional force analysis

Table 2. Barehull hydrostatic parameters for DTMB Model 5613-1 (Bassler, et al., 2007)

Displacement	260.14 kg
Draft	0.172 m
Lpp	4.8125 m
Beam	0.5875 m
KG	0.172 m
Roll Gyradius/Beam	0.361
Scale Ratio	32

EFFECTS TO CONSIDER FOR A SHIP MANEUVERING IN WAVES

Several physical effects were examined which are relevant to modeling a ship maneuvering in waves. These included 3D, forward speed, waves, maneuvering, and large amplitude roll effects. Each of these effects were examined individually, to assess their relative significant to the forces observed on the bilge keel.

Table 3. Simulated conditions for DTMB Model 5613-1

Froude Number	Roll Frequency (rad/s)	Motion Amplitude (deg)	Sea Conditions
0.0, 0.30	2.85	1-DoF Roll: 15, 25, 30, 35	Calm Water
0.0	2.85	1-DoF Roll: 25, 35	Beam Waves ($\lambda/L = 1.57$, $H/\lambda = 1/100$)
0.3	0	1-DoF Yaw: ± 10	Calm Water

3D Effects

URANS simulations were performed for the 3D ONR Tumblehome hull undergoing 1DoF forced roll oscillations at both zero and forward speed conditions, in calm water.

URANS simulations were performed for the 2-D midship section undergoing 1-DoF forced roll oscillations. Comparisons are shown between the 2-D URANS and 2-D experiment, as well as the midship section of the bilge keel force URANS results for the 3-D hull form at zero speed in calm water (Fig. 8). Comparisons were made to the experimental results of Bassler, et al. (2010b). The distinct physical processes occurring during roll motion, as observed from the experimental measurements, were given in (Bassler, et al., 2010b).

As shown, the bilge keel force results from the simulations and the experiments agreed well for roll amplitudes of 15 and 25 deg. However, for larger roll angles (30 and 35 deg), where the bilge keel interacts with and emerges from the free surface, some discrepancies are observed between the simulations and the experiments. The comparisons were made between filtered experimental results and unfiltered numerical results. Due to mechanical noise in the experimental results, filtered results for the measured bilge keel force are presented (Bassler, et al. 2010b). For the large roll amplitudes, the general shape and peak values agree well for the 2-D midship section. However, the URANS simulations have more noise for the large amplitude cases, likely due to the finite difference method used for the simulations, where emergence and re-entry of the bilge keel results in nonlinearities in the instantaneous wetted portion of the bilge keel, including water run-off, entrained air collapse, and impulse loading from their emerging and immerging from the free-surface.

For roll amplitudes up to 30 deg, at zero speed, the differences between the 2-D and 3-D midship section cuts of the bilge keel force are small. For the 35 deg case, distinct differences occur between the 2-D and 3-D results for the portion of the roll cycle where the bilge keel is emerging and then re-entering the free surface. This is likely due to 3-D effects along the bilge keel due to the flow along chord, while the 2-D case does not have any longitudinal variation along the bilge keel during large amplitude roll motions.

Forward Speed Effects

URANS results are also presented to examine the influence of forward speed (Fn = 0.3 vice Fn = 0.0) on the midship section bilge keel force (Fig. 9). As observed, even for smaller amplitude roll motion, the differences in the unit bilge keel force are greater due to forward speed effects than due to 3-D effects. Overall, the greatest difference due to forward speed occurs during the peak of the roll cycle just after the bilge keel is fully submerged. For the portion of the roll cycle where the bilge keel is near the free surface, the zero and forward speed results agree quite well. This is likely due to the shedding of vorticity from the bilge keel at the fully submerged position in the roll cycle, and the reduction in force on the bilge keel due to the vortex when it is convected downstream in the forward speed condition. For the 25 and 30 deg roll cases, the difference in the bilge keel force at the peak of the roll cycle for zero and forward speed becomes larger. This is due to the interaction of the bilge keel with the free surface, and again the bilge keel force is less for the forward speed condition than for the zero speed condition, due to the downstream convection of vorticity. For the 35 deg roll case, the portion of the roll cycle corresponding to the emergence of the bilge keel agrees well between the zero speed and forward speed conditions. For this case, the impulse loading on the bilge keel during re-entry is significant during at both speeds. However, the influence of "water shipping" (or lingering) on the topside of the bilge keel is reduced for the forward speed case, compared to the zero speed case.

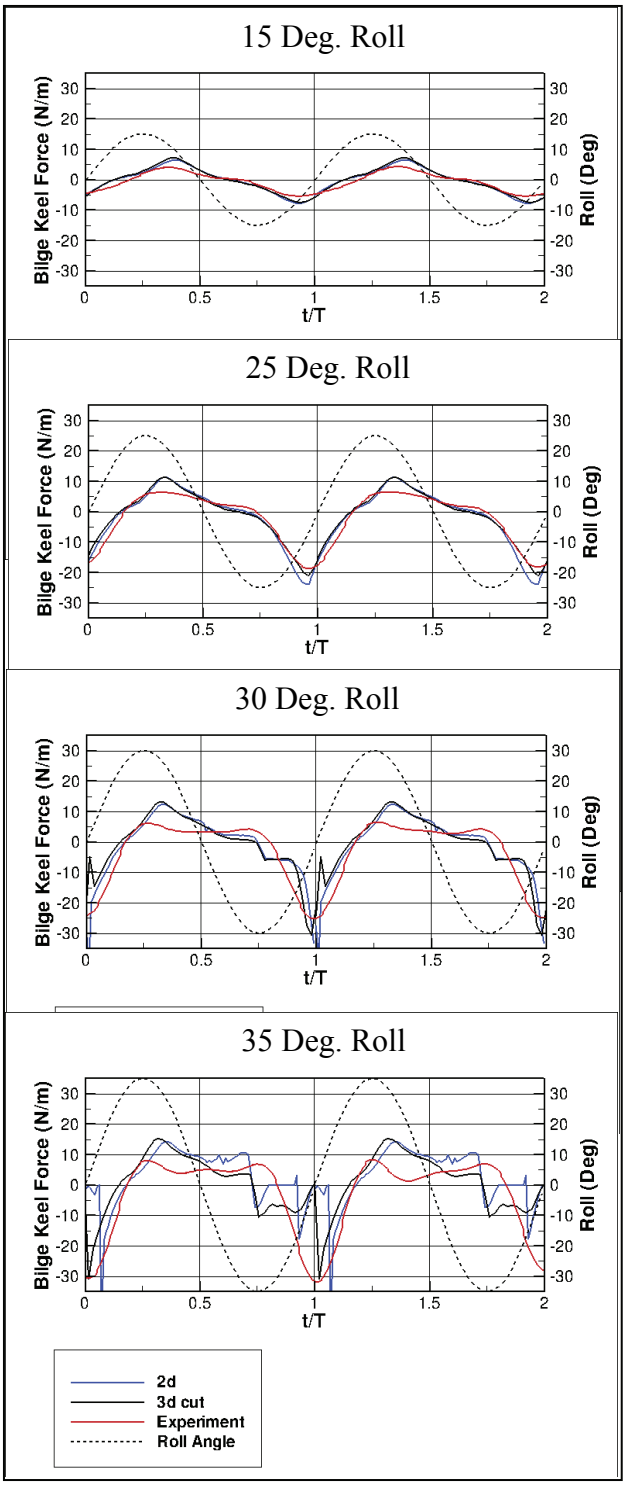

Fig.8. Bilge keel force comparisons between 2-D (solid blue) and 3-D midship section cut (solid black) URANS simulations for DTMB Model 5613-1 and 2-D model experiments (solid red) at *Fn* = 0.0, ω = 2.85 rad/s, for ϕ = 15, 25, 30 and 35 deg roll

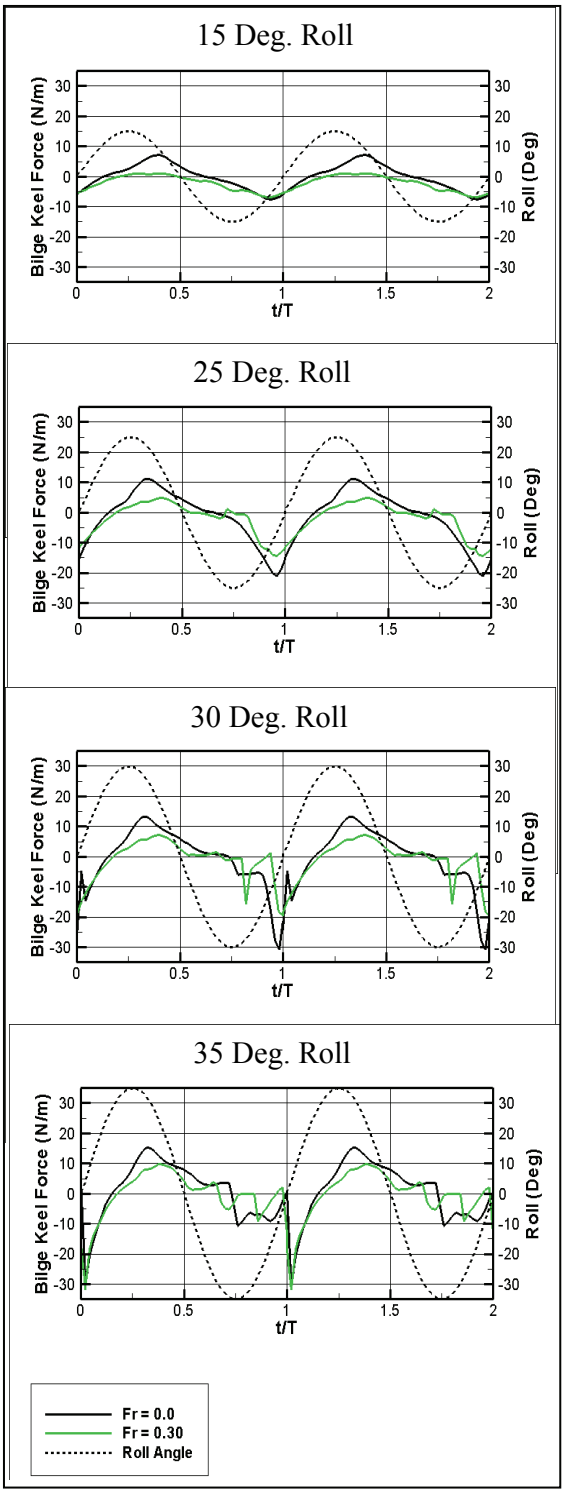

Fig. 9. Bilge keel force comparisons between 3-D URANS simulations for zero speed (solid black) and forward speed (solid green) for the midship section of DTMB Model 5613-1 at ω = 2.85 rad/s, for ϕ = 15, 25, 30 and 35 deg roll

Results are also presented for both axial vorticity and bilge keel force at various longitudinal locations along the hull, for both speeds. As shown in Fig. 10, during roll motion the vortices shed from the bilge keels and bow dome remain clustered near their shed position for zero speed.

As expected, at forward speed, the vortices are convected downstream. Near the midship section, the magnitude of the vorticity is reduced with forward speed, compared to zero speed, but also the presence of the bow-dome vortices are observed (Fig. 11).

Vorticity and bilge keel forces were examined at four specific locations, to determine the longitudinal variation for each. These locations included the leading edge (LE) of the bilge keel, and forward (x/L = 0.4), midship (x/L = 0.5) and aft (x/L = 0.6) positions on the bilge keel (Fig. 12).

For 25 deg roll at zero speed (Fig. 13), all of the positions experience similar forces, and the force variation over a roll cycle is fairly small. However, for forward speed, the leading edge force differs significantly from that at the other three positions, especially for the portion of the roll cycle where the bilge keel is near to the free surface. The maximum force appears just before the maximum upward angular velocity (t/T = 0.5). For the maximum downward angular velocity, for large angles, free-surface re-entry effects occur due to the re-wetting of the leading edge of the bilge keel with the combination of the bow wave generated by the ship at forward speed.

This significant variation for the leading edge bilge keel section is because of the pressure differentials which exist at the leading edge at forward speed, corresponding to greater lift generated at the leading edge section. This is even further exacerbated for a low aspect ratio airfoil (such as a bilge keel). The variation between the forward, midship, and aft sections is also more significant than for the zero speed condition. The effect of re-entry after emergence of the bilge keel is more pronounced for the forward speed condition.

As seen from the bilge keel forces for 35 deg roll (Fig. 14) at zero speed, the forward, midship, and aft bilge keel sections do not have significant variations. Again, even for the zero speed condition, the leading edge section of the bilge keel has a more significant impact load on re-entry then for the other sections. This may be due to the pressure differential on the bilge keel at an even higher angle of attack of the leading edge, as it follows the streamline along the hull. For the forward speed condition, significant variation is observed for the bilge keel force between the leading edge section and the other three sections. Similar to the 25 deg roll case, the bilge keel force on the leading edge section is larger for the portion of the roll cycle where the bilge keel is near to, and emerging from, the free surface. For the forward speed condition, the forward section, instead of the leading edge, of the bilge keel experienced the most significant impact loading on re-entry. This is due to the bow wave generated along the hull at forward speed, which reduced the disturbance of the bilge keel force on the leading edge section, even for the occurrence of large amplitude roll.

Wave Effects

URANS simulations were also performed for the 3-D ONR Tumblehome hull undergoing 1-DoF forced roll oscillations, at zero speed, in beam seas regular waves, with $H/\lambda = 1/100$ and $\lambda/L = 1.0$. The ship was fixed in sinkage and trim to enable more direct comparisons with the calm water forced roll oscillation conditions. The waves impacted the hull from the port side and the variation in the force on the midship section of the bilge keel, was examined, as a function of wave phase

Four comparisons, based on the wave phase relative to the peak of the roll cycle, are shown for both the 25 and 35 deg forced roll oscillation conditions. These included when the wave crest (max), wave trough (min), front slope of the wave (front) and back slope of the wave (back), coincided with the port side bilge keel at the peak (maximum) of the forced roll cycle, Figs. 15--18, respectively. As shown in the plots, the synchronization between the wave and roll frequencies occurred at t/T = 0.75, when the port side bilge keel is closest to the free surface (the maximum of the roll cycle).

For the maximum condition, where the peak of the roll cycle corresponds to the wave crest, the force on the bilge keel varies least, since it remains submerged the longest. In this case, due to re-entry effects, the 35 deg (larger) roll amplitude

results in greater force, than the 25 deg (smaller) roll amplitude, where the bilge keel remains submerged.

For the minimum condition, where the peak of the roll cycle corresponds to the trough of the wave, significant force on the bilge keel is observed due to impact loading on re-entry. In this condition, the peak force is largest, due to the higher relative velocity between the bilge keel and the free-surface---the bilge keel has greater velocity at re-entry. However, the peak force for the 35 deg case is slightly less because of the phase lag (and thus reduced time in the roll cycle) before re-entry.

For the condition with the peak of the roll cycle corresponding to the front slope of the wave (midway between crest and trough), the 25 deg case has a reduced peak force because the bilge keel does not experience emergence. However, the 35 deg case shows impact loading due to emergence of the bilge keel. This is reduced compared to the back slope of the wave, due to the direction of the orbital velocities within the wave relative to the motion of the bilge keel.

For the condition with the peak of the roll cycle corresponding to the back slope of the wave (midway between trough and crest), both the 25 deg and 35 deg cases show large peak forces on the bilge keel, due to the relative velocity on the bilge keel at re-entry.

Maneuvering Effects

The effects of coupled motions in waves, including large roll motions, while also maneuvering, are important. Previous work has shown that the vortex shedding and cross-flow drag effects on the bilge keels during steady turning, even at only small heel angles, is already significant (Dai, et al., 2009).

To examine the significance of cross-flow drag forces on the bilge keel, a series of URANS simulations were performed for the case of ±10 deg steady drift in calm water at forward speed. As seen from the pressure contours observed on the hull for windward (+10 deg) and leeward (-10 deg) drift conditions (Fig. 19), the bow dome experiences the largest pressure gradient, while the bilge keels also experience large pressure gradients at the leading edge of the windward side bilge keel (going into the flow). Meanwhile, the leeward side bilge keel is effectively sheltered by the hull. This is manifested in the longitudinal force distribution along the port side bilge keel for windward and leeward side conditions (Fig. 20). When the bilge keel is in the windward condition, a large force results on the leading edge, but is relatively constant along the remainder of the bilge keel, before tapering off at the trailing edge. When the bilge keel is on the leeward side, the sheltering by the hull results in almost no cross-flow drag force on the bilge keel.

Large Amplitude Roll Motion Effects

For large amplitude roll conditions, the bilge keel may emerge from the water, resulting in lingering forces due to water-shipping effects and severe impact loading-type behavior due to re-entry during the roll motion. These abrupt changes may create difficulty for time-domain simulation of these types of motions in potential flow codes. Additional consideration must be given to how vorticity calculations will be re-started, how the bilge keel will be de/re-wetted upon emergence and re-entry, how hysteresis effects due to “water shipping” will be considered.

In previous studies of possible models for the transition behavior of the bilge keel during emergence and re-entry by the authors, analytical formulations using methods such as a step-function, Gompertz function, or generalized logistic function (Richard’s curve) were considered. However, the semi-empirical nature of specifying coefficients for these models led them to be less than ideal for practical implementation in a robust potential flow simulation tool. Potential Flow Simulations

From the decomposition of the physical effects for consideration in modeling the bilge keel forces during ship maneuvering in waves, several aspects were examined. These included 3-D, forward speed, wave, maneuvering (cross-flow drag due to steady drift), and large-amplitude roll motion effects. From the URANS simulations, the relative importance (greatest to least) of these physical effects was assessed and is summarized as follows: forward speed, large amplitude roll, wave effects, maneuvering, 3-D effects/longitudal variation along the bilge keel.

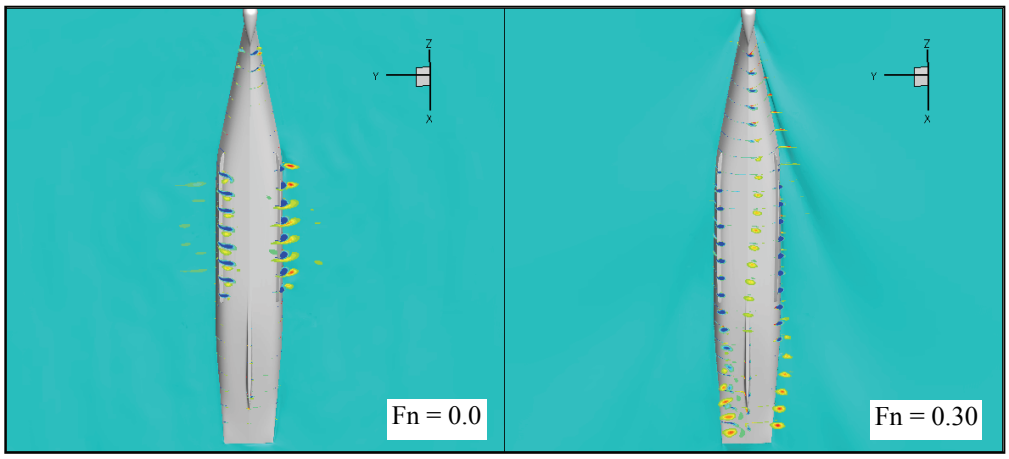

Fig. 10. Axial vorticity for DTMB Model 5613-1 at various longitudinal locations, for zero speed (left) and forward speed (right) conditions, ϕ = 25 deg, ω = 2.85 rad/s

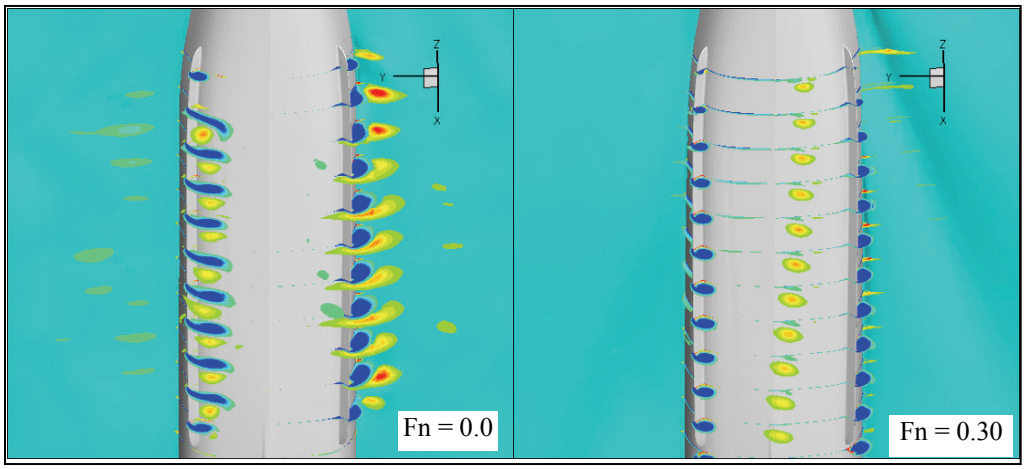

Fig. 11 Axial vorticity along the bilge keels of DTMB Model 5613-1, for zero speed (left) and forward speed (right) conditions, ϕ = 25 deg, ω = 2.85 rad/s

Forward speed convects vorticity downstream, but zero (or low) speed allows the vorticity to linger near the bilge keels, which may be difficult for potential flow simulations to capture, due to interaction effects. Other forward speed issues such as the influence of vortex shedding from the sonar dome on the bilge keels must also be considered. Bilge keel vortices will convect downstream, possibly into the shafts, skeg, and finally propulsion and rudder sections fo the hull, depending on the present ship orientation (roll, drift angle, rates, etc). An example of this for the bare hull with bilge keels, at Fn = 0.3, is given in Fig. 10. Accurate prediction of the vortices created by the bilge keels and the prediction of their interactions with other sections of the ship geometry are important

Relative Importance and Implications for Potential Flow Simulations

Large amplitude roll motion may result in the biggest reduction in bilge keel performance while the ship is maneuvering in waves. Jumps in forces caused by bilge keel interaction with the free surface may also cause computational difficulties due to discontinuities across time-steps in potential flow simulations.

Wave effects were examined and wave phase was shown to have a significant effect on the bilge

keel force, particularly when coupled with large amplitude roll motion, where the bilge keel may interact with the free surface during emergence and re-entry. Because of the variation in relative velocity between the bilge keel and the free surface, the peak loading on the bilge keel varies significantly with the phase of the motion relative to that of the wave.

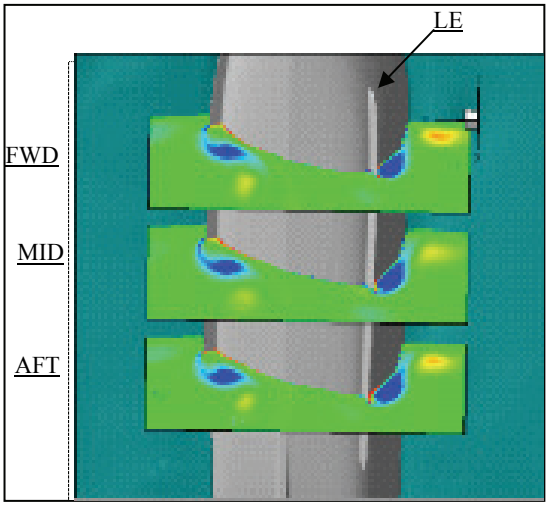

Fig.12 Locations of bilge keel force sectional analysis: leading edge (LE), forward section (at x/L = 0.4), midship section (at x/L = 0.5), and aft section (x/L = 0.6)

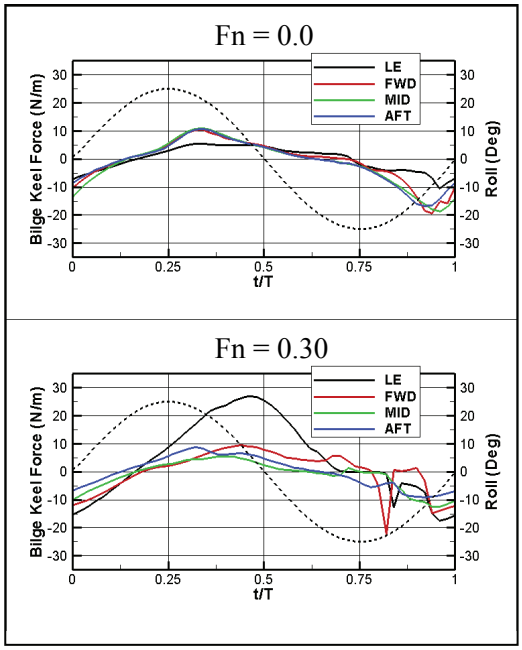

Fig.13. Unit bilge keel force for DTMB Model 5613-1, at leading edge (black), forward (red), midship (green), and aft (blue) locations, for zero speed (top) and forward speed (bottom) conditions, ϕ = 25 deg, ω = 2.85 rad/s

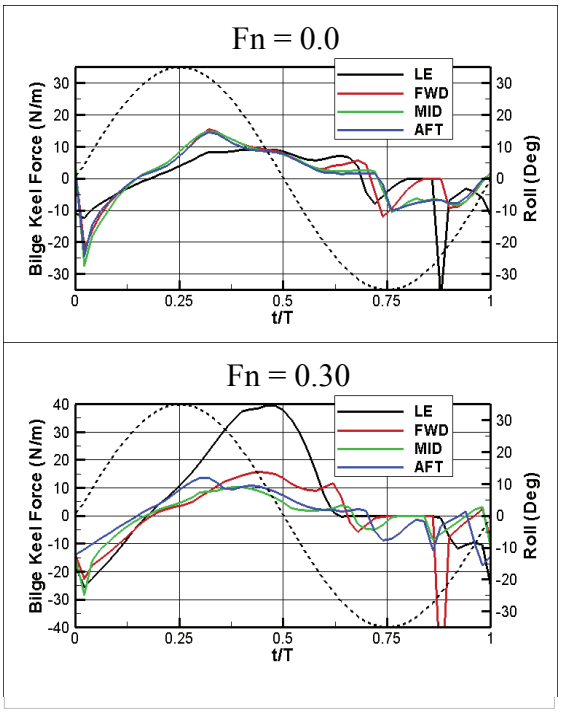

Fig. 14. Unit bilge keel force for DTMB Model 5613-1, at leading edge (black), forward (red), midship (green), and aft (blue) locations, for zero speed (top) and forward speed (bottom) conditions, ϕ = 35 deg, ω = 2.85 rad/s

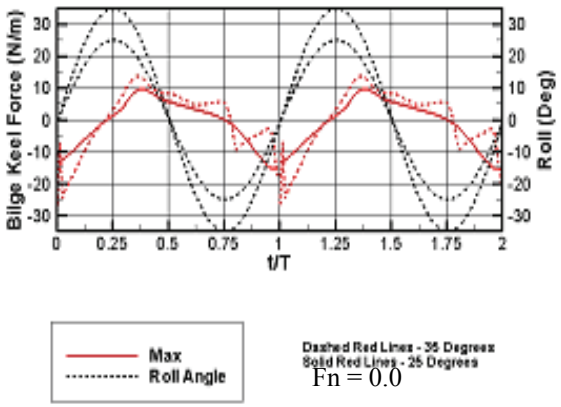

Fig. 15. Force on the midship section of the port side bilge keel for 25 (solid) and 35 (dotted) deg roll. Wave phase with crest corresponding to peak of the roll cycle (at t/T = 3/4).

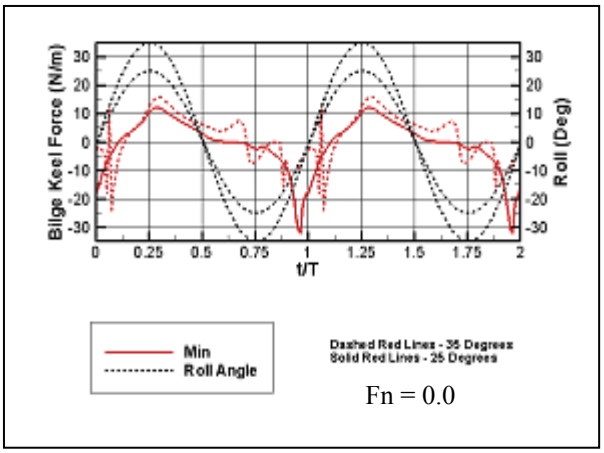

Fig.16. Force on the midship section of the port side bilge keel for 25 (solid) and 35 (dotted) deg roll. Wave phase with trough corresponding to peak of the roll cycle (at t/T = 3/4).

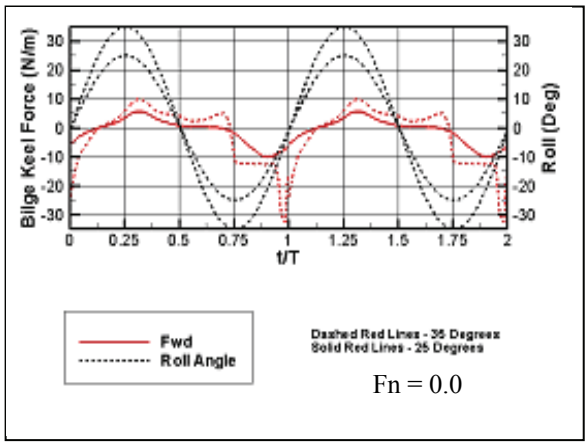

Fig. 17. Force on the midship section of the port side bilge keel for 25 (solid) and 35 (dotted) deg roll. Wave phase with front slope corresponding to peak of the roll cycle (at t/T = 3/4).

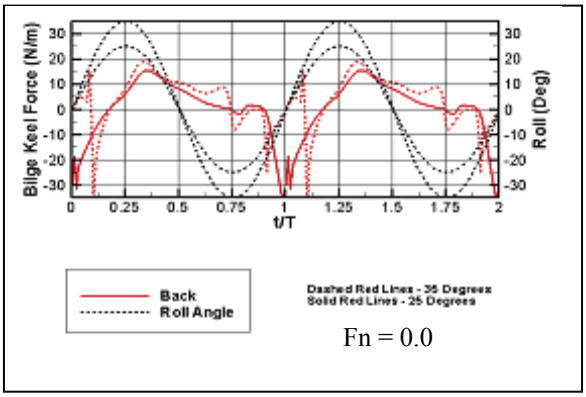

Fig.18. Force on the midship section of the port side bilge keel for 25 (solid) and 35 (dotted) deg roll. Wave phase with back slope corresponding to peak of the roll cycle (at t/T = 3/4).

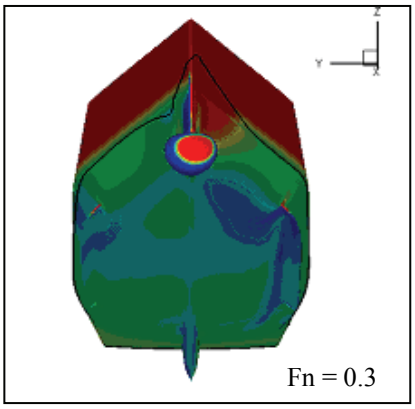

Fig. 19. Pressure contours on the submerged portion of ONRTH, for drift from the windward side (+10 deg), looking aft from the bow.

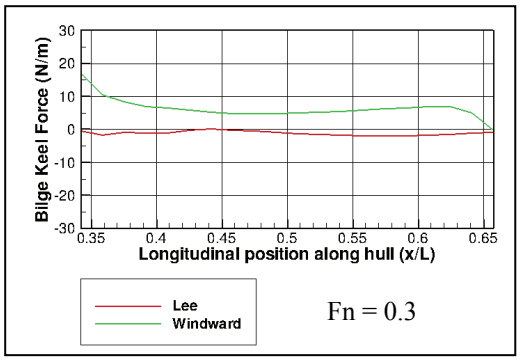

Fig. 20. Longitudinal distribution of force along the port side bilge keel for drift from the windward and leeward sides (±10 deg)

Relative Importance and Implications for Potential Flow Simulations

Large amplitude roll motion may result in the biggest reduction in bilge keel performance while the ship is maneuvering in waves. Jumps in forces caused by bilge keel interaction with the free surface may also cause computational difficulties due to discontinuities across time-steps in potential flow simulations.

Wave effects were examined and wave phase was shown to have a significant effect on the bilge keel force, particularly when coupled with large amplitude roll motion, where the bilge keel may interact with the free surface during emergence and re-entry. Because of the variation in relative velocity between the bilge keel and the free surface, the peak loading on the bilge keel varies significantly with the phase of the motion relative to that of the wave.

Maneuvering imparts a significant force on the leading edge of the windward side bilge keel, and

is important for consideration due to the impact of the inflow conditions on the bilge keel for computation of the vortex shedding in ULS methods for the bilge keel force.

From the cases examined, the 3-D effects on the bilge keel, aside from the leading edge, did not appear to be significant. Sectional formulations can be used for the bilge keel force, but care must be taken to account for forward speed, large amplitude roll, and maneuvering effects as they impact the forces on the leading edge of the bilge keel.

Morison-equation based approaches do not consider these 3-D effects, aside from the possibility of altering the coefficients at each time-step based on some pre-determined specification related to forward speed, location along the bilge keel, angle of attack to the local flow, etc . A blended approach (coupling Morison equation to a ULS method for forward speed), as proposed by Greeley & Petersen (2010), may help to address this issue. However, a blended approach will likely still have difficulties with re-wetting the sectional bilge keel geometries for large amplitude roll motions and re-starting the vorticity calculation after bilge keel re-entry has occurred. Particularly at low speed, where the trade-off between the ULS model and the Morison-equation based model occurs, and where vorticity is not being convected downstream as quickly. Under these conditions, the determination of the bilge keel force in a potential flow simulation will be difficult.

CONCLUSIONS

The purpose of this study was to assess effects which may need to be considered in future developments of force-component models for bilge keels. The comparisons performed for this study enabled the examination of effects due to vortex shedding, flow convection downstream, waves, maneuvering and bilge keel emergence and immergence during large roll motion. This investigation led to improved understanding of the effects which should be considered for sectional, or strip-theory based, approaches for ship motion predictions.

For the single hull form, bilge keel configuration, wave condition, and drift condition that were examined, for two speeds, the following observations were made:

- 2-D results from URANS and experiments generally agreed, even for large amplitude roll motion, although differences were likely due to the limitations of finite difference methods used in the URANS simulations
- 3-D effects were more significant for zero speed conditions, but were also apparent for the forward speed condition, where vorticity is convected downstream
- The effects of vorticity on the bilge keel force were reduced with forward speed; however, at forward speed an additional component from the bow dome was present and may have some influence on the bilge keel force for lower frequency oscillations
- At zero speed, there is not much longitudinal variation in the bilge keel force, except for the re-entry of the leading edge section for large amplitude roll
- At forward speed, lift and free surface effects (near to and emerging from) are greatest for the leading edge section
- At forward speed, the bow wave influences the location and magnitude of the impact loading on the bilge keel
- The presence of waves influences the force on the bilge keel, and depends on the phase of the wave relative to the roll cycle; while the bilge keel is deeply submerged, the influence of the waves is least.
- For large amplitude roll conditions in waves, when the bilge keel emerges from the free surface, the magnitude of the impact loading on the bilge keel during re-entry is reduced.
- The effect of different wave phases on the bilge keel force, such as bilge keel re-entry in a wave trough, which may lead to an increase in the bilge keel force compared to calm water and compared to other wave phases.
- In calm water, the effect of steady drift on the bilge keel forces was examined. The more complex conditions of unsteady turns in waves, while experiencing large amplitude coupled motions should be considered for future study.

Interactions of the vortices shed from the bilge keels may be significant, particularly for stability

failure conditions. For these conditions, steep waves may result in large amplitude roll motions, while the ship is typically moving at slower speeds, or is in a dead ship condition, and the vortices will have a lingering presence. At zero or slow speeds, the influence of the vorticity may be more difficult to consider in sectional or strip-theory based approaches for ship motion predictions. Additionally, for more advanced bilge keel designs, including tip geometry variations, consideration must be given to the effects of bilge keel geometry on damping.

Future development of bilge-keel force-component models for potential flow ship motion simulations should consider forward speed effects.

Additional comparisons between the URANS results obtained in this study and the computationally efficient bilge keel force model proposed by Greeley & Petersen (2010) are planned.

The development of more physically robust bilge keel force models may enable more unconventional bilge keel designs to be evaluated. This will allow future numerical tools to evaluate ship designs with variations in bilge keel geometries to improve roll damping performance in sea conditions, including heavy weather.

ACKNOWLEDGEMENTS

The authors would like to thank Dr. Pat Purtell (Office of Naval Research) for support of the work presented in this paperand acknowledge support for the experiments and additional analysis from the NSWCCD Independent Applied Research (IAR) Program, under the direction of Dr. John Barkyoumb. They appreciate Dr. Pablo Carrica (University of Iowa) for his continued guidance and support in using CFDShip-Iowa. They are grateful to the U.S. Department of Defense's High Performance Computing Modernization Program (HPCMP) office, which provided the computer resources at NAVO on the IBM P6.

REFERENCES

Atsavapranee, P., J. B. Carneal, D. Grant, & A. S. Percival (2007), "Experimental Investigation of Viscous Roll Damping on the DTMB Model 5617 Hull Form," Proc. 26th Intl. Conf. on Offshore Mechanics and Arctic Eng, San Diego, CA.

Bassler, C., J. Carneal & P. Atsavapranee (2007) "Experimental Investigation of Hydrodynamic Coefficients of a Wave-Piercing Tumblehome Hull Form," Proc. 26th Intl. Conf. Offshore Mechanics and Arctic Engineering, San Diego, CA.

Bassler, C. C. & A. M. Reed (2009) "An Analysis of the Bilge Keel Roll Damping Component Model," Proc. 10th Intl. Conf. Stability of Ships and Ocean Vehicles, St. Petersburg, Russia.

Bassler, C. C., A. M. Reed, & A. J. Brown (2010a), "A Method to Model Large Amplitude Ship Roll Damping," Proc. 11th Intl. Ship Stability Workshop, Wageningen, The Netherlands.

Bassler, C. C., A. M. Reed, & A. J. Brown (2010b), "Characterization of Physical Phenomena for Large Amplitude Ship Roll Motion," Proc. 29th American Towing Tank Conf. (ATTC), Annapolis, MD, August.

Bassler, C. C., A. M. Reed, & A. J. Brown (2011) "A Piecewise Model for Prediction of Large Amplitude Ship Roll Damping," Proc. 30th Intl. Conf. Ocean, Offshore and Arctic Eng, Rotterdam, The Netherlands, June.

Beck, R. F. & A. M. Reed (2001) "Modern Computational Methods for Ships in a Seaway," Trans. SNAME, 109, pp. 1–51.

Belknap, W. & A. M. Reed (2010), "TEMPEST: A New Computationally Efficient Dynamic Stability Prediction Tool," Proc. 11th Intl. Ship Stability Workshop, Wageningen, The Netherlands.

Belknap, W., C. Bassler, M. Hughes, P. Bandyk, K. Maki, D. H. Kim, R. Beck, & A. Troesch (2010), "Comparisons of Body-Exact Force Computations in Large Amplitude Motion," Proc. 28th Symp. on Naval Hydro., Pasadena, CA,.

Bishop, R. C., W. Belknap, C. Turner, B. Simon, & J. H. Kim (2005), "Parametric Investigation on the Influence of GM, Roll Damping, and Above-Water Form on the Roll Response of Model 5613," Hydromechanics Dept. Technical Report, NSWCCD-50-TR-2005/027.

Boger D.A & J. J. Dreyer J.J. (2006), "Prediction of Hydrodynamic Forces and Moments for Underwater Vehicles Using Overset Grids," Proc 44th AIAA Aerospace Sciences Meeting, Reno, Nevada.

Bryan, G. H. (1900), "The Action of Bilge Keels," Trans. RINA 4.

Carrica P. M., R. V. Wilson, R. Noack, T. Xing, M. Kandasamy, J. Shao1, N. Sakamoto, & F. Stern

(2006), "A Dynamic Overset, Single-Phase Level Set Approach for Viscous Ship Flows and Large Amplitude Motions and Maneuvering," Proc 26th Symp. on Naval Hydro., Rome, Italy.

Carrica, P.M., R. V. Wilson, R. W. Noack, & F. Stern, (2007a), "Ship Motions Using Single-Phase Level Set with Dynamic Overset Grids," Computers and Fluids, 36, pp. 1415-1433.

Carrica, P.M., R. V. Wilson, & F. Stern (2007b), "An Unsteady Single-Phase Level Set Method for Viscous Free Surface Flows," Intl. J. Numerical Methods in Fluids, 53, pp. 229-256.

Dai, C.M., Miller, R.W, & Percival A.S. (2009), "Hydrodynamic Effects of Bilge Keels on the Hull Flow During Steady Turns," Proc. 28th Intl. Conf. Ocean, Offshore and Arctic Engineering, Honolulu, Hawaii.

Froude, W. (1865), "On the Practical Limits of the Rolling of a Ship in a Seaway," *Trans. Institution of Naval Architects*, 6.

Grant, D. J., A. Etebari, & P. Atsavapranee (2007), "Experimental Investigation of Roll and Heave Excitation and Damping in Beam Wave Fields," *Proc. 26th Intl. Conf. on Offshore Mechanics and Arctic Engineering*, San Diego, CA.

Greeley, D. S. & B. J. Petersen (2010), "Efficient Time-Domain Computation of Bilge Keel Forces,"*Proc. 28th Symp. on Naval Hydro.*, Pasadena, CA, September.

Ikeda, Y., Y. Himeno, & N. Tanaka (1978), "A Prediction Method for Ship Roll Damping," Report of the Department of Naval Architecture, University of Osaka Prefecture, No. 00405.

Irvine, M., P. Atsavapranee, J. Carneal, A. Engle, S. Percival, R. Bishop, D.Grant, C. Lugni, F. Di Felice, J. Longo, & F. Stern (2006), "Comparisons of Free Roll Decay Tests for Model DTMB 5415/2340/5512, and Investigation of Lateral Hydrodynamic Loads on Bilge Keels," Proc. 26th Symp. on Naval Hydro., Rome, Italy,.

Himeno, Y. (1981), "Prediction of Ship Roll Damping-State of the Art," Dept. of Naval Architecture and Marine Engineering, Univ. of Michigan, Report 239.

Kato, H. (1965) "Effect of Bilge Keels on the Rolling of Ships." J. Soc. Naval Arch., Japan, 117, pp. 93–114.

Keulegan, G. M. & L. H. Carpenter (1958), "Forces on Cylinders and Plates in an Oscillating Fluid," J. Research of the National Bureau of Standards, 60.

Klaka, K., J. D. Penrose, R. R. Horsley, & M. R. Renilson (2007), "Hydrodynamic Tests on a Plate in Forced Oscillation," Ocean Engin., 34, pp. 1225-1234.

Korpus, R. A. & J. M. Falzarano (1997), "Prediction of Viscous Ship Roll Damping by Unsteady Navier-Stokes Techniques," J. Offshore Mech. & Arctic Engin., 119, pp. 108-113.

Lin, W. M., & D.K.P. Yue (1990), "Numerical Solutions for Large-Amplitude Ship Motions in the Time-Domain," Proc. 18th Symp. Naval Hydro., Ann Arbor, MI.

Lin, W. M., S. Zhang, K. Weems, & D. Liut (2006), "Numerical Simulations of Ship Maneuvering in Waves," Proc. 26th Symp. Naval Hydro., Rome, Italy.

Liut, D. A. (1999), Neural-Network and Fuzzy-Logic Learning and Control of Linear and Nonlinear Dynamic Systems, Ph.D. Dissertation, Virginia Tech.

Liut, D. A. & W.M. Lin (2006), "A Lagrangian Vortex-Lattice Method for Arbitrary Bodies Interacting with a Linearized Semi-Lagrangian Free Surface," Intl. Shipbuilding Progress, 53, pp. 1-32.

Lloyd, A. R. J. M. (1998), Seakeeping: Ship Behaviour in Rough Weather. London: Intl. Book Distributors, Ltd.

Martin, M. (1958) "Roll Damping Due to Bilge Keels." U. Iowa Institute of Hydraulic Research, Report.

Menter, F. R. (1994), "Two-Equation Eddy Viscosity Turbulence Models for Engineering Applications," *AIAA J.*, 32, pp. 1598-1605.

Miller, R. W., J. J. Gorski, & D. Fry (2002), "Viscous Roll Predictions of a Circular Cylinder with Bilge Keels," Proc. 24th Symp. Naval Hydro., Fukuoka, Japan.

Miller, R. W., C. C. Bassler, P. Atsavapranee, & J. J. Gorski (2008), "Viscous Roll Predictions for Naval Surface Ships Appended with Bilge Keels Using URANS," Proc. 27th Symp. Naval Hydro., Seoul, South Korea.

Morison, J. R., M. P. O'Brien, J. W. Johnson, & S. A. Schaaf (1950), "The Forces Exerted by Surface Waves on Piles," Petroleum Trans., AIME, 189, pp. 149-157.

Morison, J. R., J. W. Johnson, & M. P. O'Brien (1953), "Experimental Studies of Forces on Piles," Proc. 4th Conf. Coastal Engin.

Noack R. (2005), "SUGGAR: A General Capability for Moving Body Overset Grid Assembly," Proc 17th AIAA Computational Fluid Dynamics Conf., Toronto, Ontario, Canada.

Reed, A. M. (2009) "A Naval Perspective on Ship Stability," Proc. 10th Intl. Conf. Stability of Ships and Ocean Vehicles, St. Petersburg, Russia.

Roddier, D., S. W. Liao, & R. W. Yeung (2000), "On Freely-Floating Cylinders Fitted with Bilge Keels," Proc. 10th Intl. Offshore and Polar Engin. Conf.

Sarpkaya, T. (1981), "A Critical Assessment of Morison's Equation and Its Applications," Proc. Intl. Conf. on Hydro. Ocean Engin., Trondheim, Norway, pp. 447-467.

Sarpkaya, T. & M. Isaacson (1981), Mechanics of Wave Forces on Offshore Structures. New York: Van Nostrand Reinhold Co.

Sarpkaya, T. & J. L. O'Keefe (1996), "Oscillating Flow Around Two and Three-Dimensional Bilge Keels," J. Offshore Mechanics and Arctic Eng, 118, pp 1-6.

Seah, R. K. M. (2007), "The SSFSRVM Computational Model for Three-Dimensional Ship Flows With Viscosity," Ph.D. Dissertation, University of California Berkeley.

Seah, R. K. M. & R. W. Yeung (2008), "Vortical-Flow Modeling for Ship Hulls in Forward and Lateral Motion," Proc. 27th Symp. on Naval Hydrodynamics, Seoul, South Korea.

Themelis, N. I. (2008), "Probabilistic Assessment of Ship Dynamic Stability in Waves," Ph.D. Dissertation, National Technical University of Athens.

Wilson, R.V., P. M. Carrica, & F. Stern, (2006), "Unsteady RANS Method for Ship Motions with Application to Roll for a Surface Combatant," Computers and Fluids, 35, pp. 501-524.

Yeung, R. W, S. W. Liao, & D. Roddier (1998), "Hydrodynamic Coefficients of Rolling Rectangular Cylinders," Intl. J. Offshore and Polar Eng, 8(4).

Yeung, R. W., D. Roddier, B. Alessandrini, L. Gentaz & S. W. Liao (2000), "On the Roll Hydrodynamics of Cylinders Fitted with Bilge Keels," Proc. 23rd Symp. on Naval Hydro

.